Mechatronics 19 (2009) 548–561

Contents lists available at ScienceDirect

Mechatronics

journal homepage: www.elsevier.com/locate/mechatronics

Sliding mode control of quadruple tank process

Pinak Pani Biswas, Rishi Srivastava, Subhabrata Ray, Amar Nath Samanta *

Department of Chemical Engineering, IIT Kharagpur, Medinipore, West Bengal 721302, India

ARTICLE INFO

Article history:
Received 14 June 2007
Accepted 13 January 2009

Keywords:
Sliding mode control
Quadruple tank
Multivariable control
Non-minimum phase system

ABSTRACT

The process investigated herein is the quadruple tank system that is stable only within a limited zone of operating parameters. The process model has been developed from fundamentals and tuned with experimental data. A controller design based on feedback linearization has been tested on this process model. Coupling feedback linearization with sliding mode algorithm provides robust control of the process and performs far superior to conventional PI control. A PC based controller interfaced to the experimental quadruple tank experimental set up has been used to implement this algorithm and test its performance. Inserting a 'boundary layer' around the sliding surface reduced the 'chattering' associated with sliding mode control. The implemented controller provides robust control and excellent set point tracking.

1. Introduction

Quite a few researchers [1–6] have worked on liquid level control of single or coupled tanks. Quadruple tank process is an example to illustrate the effect of multivariable zero locations on controller design [7]. The realization of zeros based on observable process conditions was the motivation to develop it. Johansson [8] developed a decentralized PI controller for the quadruple tank process but the right half plane zero imposes serious limitations on the performance of the controller in non-minimum phase. Johansson [8] found that for minimum phase case a decentralized controller is equally good as centralized one but for non-minimum phase case he found that controller based on H_∞ design methods gave 30–40% lower settling time compared to the responses of decentralized PI controller. Grebeck [9] tested effectiveness of centralized PI controller for quadruple tank process experimentally. Johansson et al. [10] considered the relative gain array for the quadruple tank process. They have shown that reversal of pairing from the normal leads to better operation in the non-minimum phase case. Multivariable controller tuning of quadruple tank based on relay feedback experiments was also investigated by researchers [11,12]. It was shown that many of the available multivariable tuning methods cannot handle the automatic controller design for minimum phase and non-minimum phase with equal ease and elegance [12].

Variable structure control systems [13] have gained significant attention in the last two decades. Theory for sliding mode and variable structure systems (VSS) is well documented in [14–17]. Various workers have worked to deepen the roots of sliding mode theory and coupled it with other strategies. Hseng et al. describe an evolutionary programming (EP) based fuzzy sliding mode control (FSMC) for a magnetic ball suspension system [18]. Lino et al. [19] present a control oriented model and a sliding mode control design for a common rail injection system. Iglesias et al. [20] describe a new controller based on a combination of Sliding Mode Control and Fuzzy Logic. Chen and Peng [21] consider the robust control of non-linear uncertain chemical processes in the presence of input-delay and inverse response. Their scheme can be utilized for regulation control of a non-minimum phase process and they extended it for the system having dynamics of first order with dead time. Systematic assessment of chattering problem and sliding mode control solution for real life engineering problems are well covered in literature [22]. Implementation of sliding mode strategy on a coupled system of two tanks is done by Almutairi and Zribi [23]. They have considered static sliding mode control of the process, which suffers performance degradation due to high chattering. They developed dynamic sliding mode strategy to overcome this problem. The robustness of control schemes to change in system's parameters and disturbances were also considered. Implementation of sliding mode on quadruple tank is still untouched and implementing the same can illustrate stepwise addressing of several problems of concern like estimation of bounds, parametric variation and stability.

In this paper, our objective is to address issues related to sliding mode control implementation on quadruple tank process and present an analysis of sliding mode controller design. The physical set up used for this purpose had quite a few model parameters that depend either on operating conditions or on some stochastic disturbances. Experimental validation of control performance proves that our design is indeed capable of dealing with inherent uncertainties of the model and can be a good basis for step-by-step

* Corresponding author. Tel.: +91 3222 283948.
E-mail address: amar@che.iitkgp.ernet.in (A.N. Samanta).

0957-4158/$ - see front matter © 2009 Elsevier Ltd. All rights reserved.
doi:10.1016/j.mechatronics.2009.01.001

design of multivariable sliding control strategy. The controller is designed in the difficult zone of controllability, the non-minimum phase operating zone of the process. With the objective of better control performance with constraint on manipulated variable chattering limit, a sliding mode control with a boundary layer is designed and validated on a simulated process model. Then the same is implemented on the experimental set up and its performance is evaluated.

2. Process description

The 'quadruple tank process', a combination of two double tank systems is shown schematically in Fig. 1. This setup (Model No. 327B) procured from M/s. Apex Innovations, India, is interfaced to a Pentium IV based PC via interfacing modules & serial ports. This setup consists of a water supply tank with two variable speed positive displacement pumps (capacity 0–200 lph) for water circulation fitted with flow dampers, four transparent process tanks fitted with level transmitters, rotameters. Process signals from the four tank level transmitters are interfaced with computer. Control algorithm running on the computer sends outputs to the individual pump variable frequency drive through interfacing units. Tanks 1 and 2 are mounted below the other two tanks for receiving water flow by gravity. Each tank outlet opening is fitted with a valve. Both pumps 1 and 2 take suction from the supply tank. Each pump is fitted with an air cushioned buffer tank to dampen the flow fluctuations from the metering pumps. Discharge from pump 1 is split between tank 1 and tank 4 and the flows are indicated by rotameters 1 and 4. Similarly, pump 2 splits its discharge between tank 2 and tank 3 and the split flows are indicated by rotameters 2 and 3. Split of flow from pump 1 and pump 2 can be varied by manual adjustment of valves S1 and S2. Tank 1 and tank 2 also receive gravity flow from tank 3 and tank 4, respectively. Opening of these valves (V1, V2, V3 and V4), and the flow split valves (S1 and S2) can be manually adjusted to substantially alter the characteristics of the system. What makes the process more complicated is the dependence of split fraction on pump output flow rate even at constant split valve opening. The (split) fraction of flow from a pump going to the lower tank decreases with increase in pump flow. This is a strong source of non-linearity and the process initially starting in minimum phase can transit to non-minimum phase during operation. The equipment details are shown in Table 1.

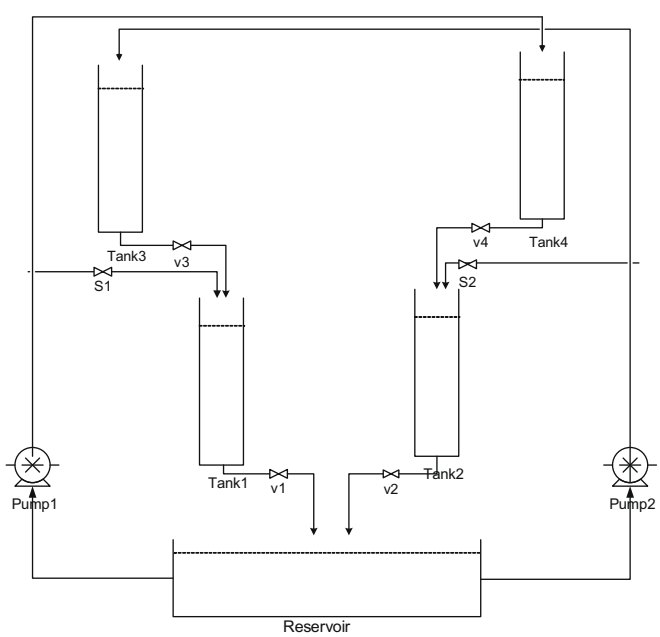

Fig. 1. Schematic diagram of the setup.

3. Model development

Achieving desired levels (set points) in tank 1 and tank 2 is the control objective. The process has two inputs – flow from pumps 1 and 2. These are set by signal inputs u_1 and u_2, which are the % output from the controller. There are four levels (h_1, h_2, h_3 and h_4) that are measured, transmitted and are available on-line for the control algorithm to make use of.

Johansson's [8] model equations can be adopted for our system by neglecting the pressure drop in the piping compared to the pressure drop in the valves:

$$\begin{aligned}
\frac{dh_1}{dt} &= -\frac{a_1}{A_1}\sqrt{2gh_1} + \frac{a_3}{A_1}\sqrt{2gh_3} + \frac{\gamma_1 k_1}{A_1}u_1 \\
\frac{dh_2}{dt} &= -\frac{a_2}{A_2}\sqrt{2gh_2} + \frac{a_4}{A_2}\sqrt{2gh_4} + \frac{\gamma_2 k_2}{A_2}u_2 \\
\frac{dh_3}{dt} &= -\frac{a_3}{A_3}\sqrt{2gh_3} + \frac{(1-\gamma_2)k_2}{A_3}u_2 \\
\frac{dh_4}{dt} &= -\frac{a_4}{A_4}\sqrt{2gh_4} + \frac{(1-\gamma_1)k_1}{A_4}u_1
\end{aligned} \tag{3.1}$$

where A_i, cross-section of tank i; a_i, open cross-section of the outlet line valve on tank j; h_i, water level in tank i; u_i, controller output signal (%) applied to pump i; $k_i u_i$, corresponding water flow rate in pump i; γ_1, split fraction for split valve 1; γ_2, split fraction for split valve 2.

Each of the valves (V1, V2, V3, V4, S1 and S2) has non-linear characteristics and they interact to increase the order of dynamics. Limits of stable (*steady state*) operation range in our set up are determined experimentally. In Fig. 2 experimental as well as sim-

Table 1
Equipment specification and component details.

Product	Multi variable level control trainer
Control unit	Interfacing unit with ADC/DAC conversion, no. of analog inputs: 4, analog outputs 1 (2nos.)
Level transmitter	Type capacitance, two wire, range 0–300 mm, output 4–20 mA (4nos.)
Rotameter	16–160 lph (4nos.)
Pump	Positive displacement dosing pump with adjustable stroke (2nos.)
Pump drive	Variable frequency drive, programmable, input 4–20 mA, output speed 150–1500 RP
Process tank	Acrylic, transparent, cylindrical with 0–100% graduated scale (4nos.)
Overall dimensions	650W × 500D × 1170H mm
Interfacing unit	Made by Cuadra, model AX-402, input 4–20 mA (4nos.), output 4–20 mA (1no.). Communication RS232
Rotameter	Made by Eureka, Model MG 12, range 16–160 lph, Connection ¼″ back, screwed, packing neoprene
VFD	Made by Integrated Electric, Model IRAC 01 M, input voltage 1 ph AC 230 V, output frequency 0–200 Hz
Dosing pump	Made by ITC Spain, Model 62-A21-D2PR, capacity 0–200 lph, pressure 6 kg/cm^2, material of construction PP, power 0.46 kW
Level transmitter	Made by Switzer, model K-5750-W-3-SK-1-R-3-E-0-1, measuring range 300 mm, output 4–20 mA, two wire isolated

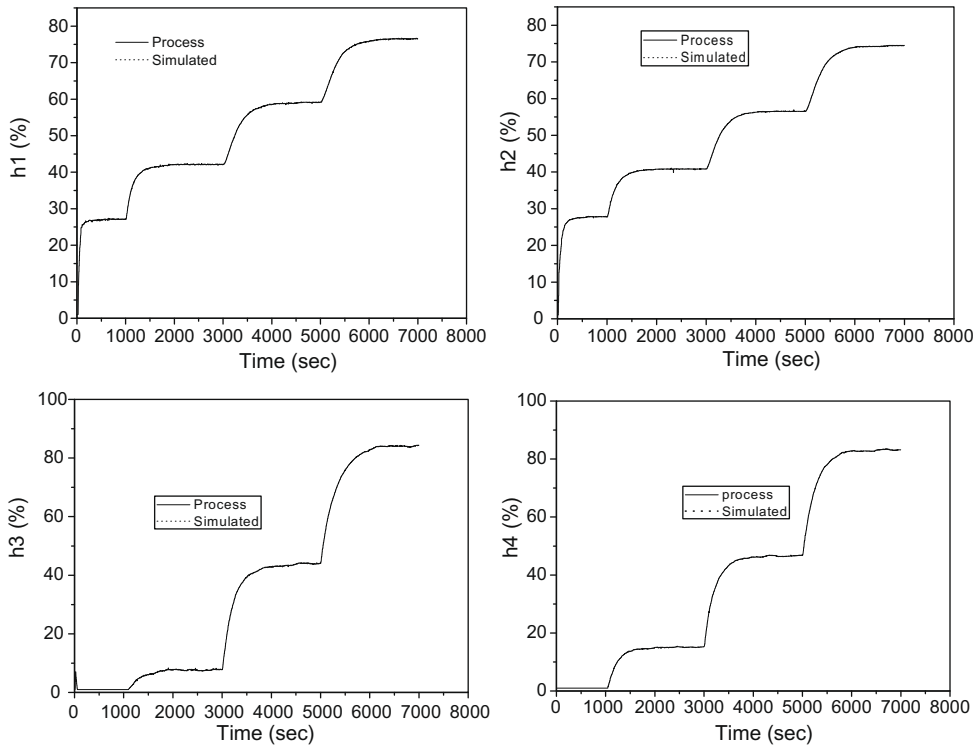

Fig. 2. Experimental observation by sequentially changing the inputs.

ulated results were recorded by sequentially changing the inputs after allowing a reasonable stabilization period. We gave a series of 10% step changes in input flow rate, starting from 40% to 70%. The operating range for manipulated variables and controlled variable for a set of typical fixed openings of all the valves are determined from the responses (h_1, h_2, h_3 and h_4). Minimum limiting values of manipulated variables were determined from the limit of almost dry out of the top two tanks and the maximum manipulated variable values were determined from overflow conditions in all the tanks. The simulated and the real process variables are quite close and the stable operating range arrived at is shown in Table 2.

In this operating zone the model equations take the concise form:

$$\begin{aligned} A_1\dot{h}_1 &= -K_1\sqrt{h_1} + K_3\sqrt{h_3} + \gamma_1 k_1 u_1 \\ A_2\dot{h}_2 &= -K_2\sqrt{h_2} + K_4\sqrt{h_4} + \gamma_2 k_2 u_2 \\ A_3\dot{h}_3 &= -K_3\sqrt{h_3} + (1-\gamma_2) k_2 u_2 \\ A_4\dot{h}_4 &= -K_4\sqrt{h_4} + (1-\gamma_1) k_1 u_1 \end{aligned} \tag{3.2}$$

where K_i's are the system parameters that we will call conductance throughout. These parameters are actually governed by the valve openings and fixing these values implies ignoring the non-linear characteristics of the valves and approximating the same by steady orifice flow equation. Under this assumption, the system is represented in Eq. (3.2).

Table 2
Operating range of the process for a typical set of valve openings.

Operating variable	Minimum value (%)	Maximum value (%)
u_1	40	65
u_2	40	65
h_1	35	80
h_2	35	80
h_3	6	90
h_4	6	90

The conductance value depends on corresponding steady state height in the tank under consideration. Steady state experiments are conducted for different u_1 and u_2 combinations within the operating range and the conductance values are estimated from flow split and level measurements. These conductance values are fitted to an arbitrary form of the equation: $K = A * \exp(h/B) + C$. Fig. 3 shows height vs. conductance curve obtained from experimental data and the fitting equation. Values of the constants A, B and C are presented in Table 3. Any error in the estimation of these conductance values and other approximations in model can be taken care of by sliding mode algorithm.

The quadruple tank process has two transmission zeros, position of which depend on values of the split fractions γ_1 and γ_2. It can be shown that

For minimum phase: $1 < (\gamma_1 + \gamma_2) < 2$

For non-minimum phase: $0 < (\gamma_1 + \gamma_2) < 1$

Physical interpretation of the mathematical condition for minimum phase is that the sum of inflow rates in top tanks are less than sum of inflow rates to the bottom tanks. This is a more controllable situation intuitively. The sum of the split fractions falling below unity will alter the characteristic from minimum phase to non-minimum phase system.

It is seen from Fig. 2 that the gain of the h_1 and h_2 is lower than that of h_3 and h_4 as the pump flow rate is increased by the same %. This implies that the split fraction also introduces non-linear dynamics to the system. Increasing pump flow rate forces higher proportion of water to the upper tank and the split fraction (gamma) decreases. The steady state level of the tank is also higher at higher pump flow rates. This is incorporated in the model by introducing a correlation between split fraction and input signal to the pump. Fig. 4 shows the variation of split fraction with input signal to the pump. The relationship is fitted to the equation $\gamma_i = a_i * \exp(b_i * u_i) + c_i * \exp(d_i * u_i)$, and the constants based on experimental data are shown in Table 4.

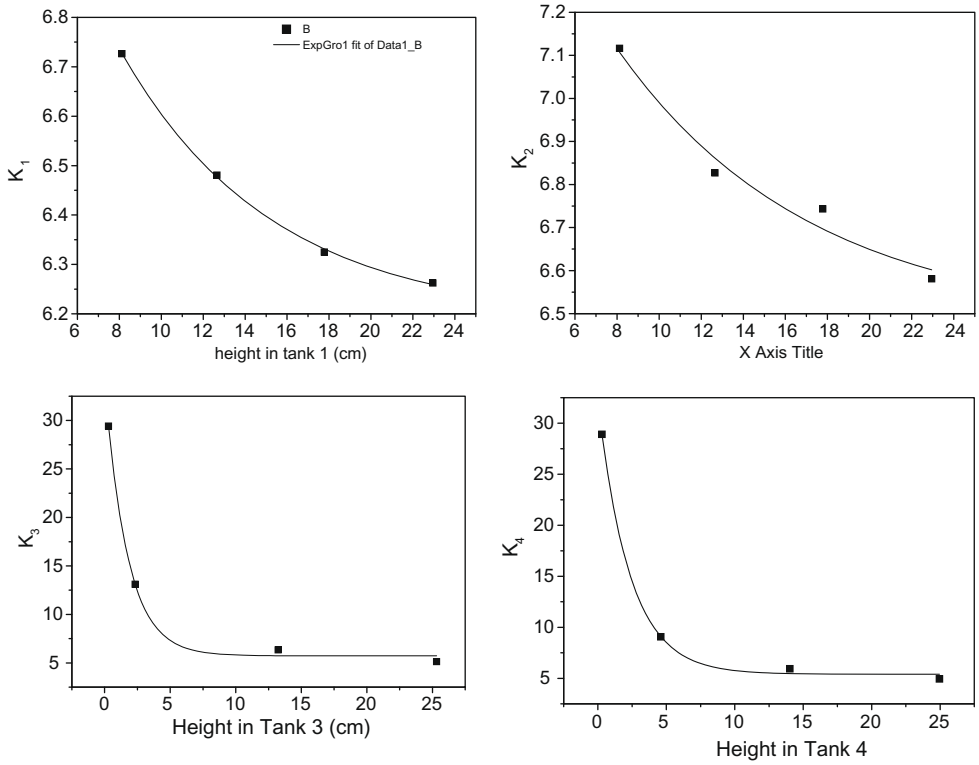

Fig. 3. Relation between conductance's and steady state height.

Table 3
Conductance estimation parameters.

Conductance	*C*	*A*	*B*
K_1	6.19076	1.65778	−7.20092
K_2	6.47688	1.52877	−9.16735
K_3	5.72611	28.1437	−1.74005
K_4	5.39772	26.74872	−2.32226

Table 4
Split fraction estimation table.

Pump no.	*a*	*b*	*c*	*d*
1	0.567	−0.1685	0.4326	−0.00534
2	0.4673	−0.0478	0.3301	−0.001858

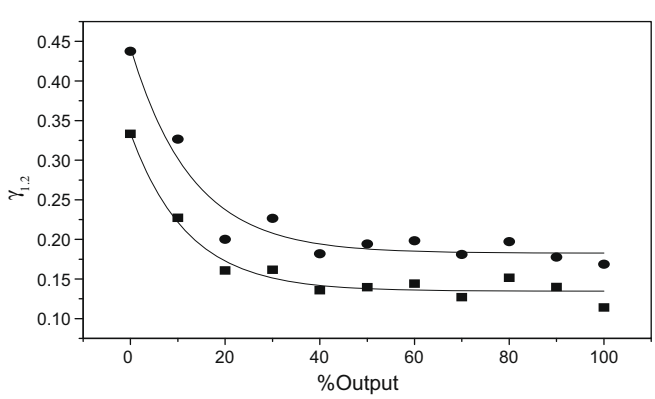

Fig. 4. Variation of split fraction (γ) vs. % output of pumps.

The γ values lie between 0.1 and 0.2 in the stable operating zone restricted by 40–65% signal to the pumps. It follows from earlier discussions that the system with this range of gamma values is in the non-minimum phase zone, i.e. the position of right half plane zero is far away in the right hand side of the origin.

In this operating range of gamma values, 80–90% of total water from the pumps goes to upper tanks leaving only a small direct flow to the lower tanks. Any change in a pump flow therefore affects the upper tank level more than the bottom one. This effect is more dominant at higher flow rate from pumps and one observes higher gain of upper tank levels compared to lower tanks. The gain also is variable, and there is a larger difference between upper and lower tank gains at higher pump flow rates. This system with severe non-linearity is therefore operable only in a narrow stable zone with non-minimum phase conditions.

Validation of model is done experimentally. The results of experimental observation and simulation are shown in Fig. 5. In order to validate over the entire operating range, the manipulated variables are initially set to their minimum initially and the process is allowed to attain steady state. Step changes in manipulated variables are imposed after the attainment of steady state and again the process is allowed to settle to a new steady state. This procedure is repeated unless we get overflow in some of the tanks. The response in the case where we have overflow is discarded. It can be seen from Fig. 5 that the simplifying assumptions and model mismatches lead to steady state deviations between simulated and actual process but the nature of transients are similar.

This process offers the challenge of developing a suitable robust non-linear controller for meeting the control objective of controlling the lower tank levels by manipulating the pump flow rates. The sliding mode control algorithm is systematically applied for designing a controller for the quadruple tank system in the region of non-minimum phase i.e. $0.1 \leqslant \gamma_1, \gamma_2 \leqslant 0.20$.

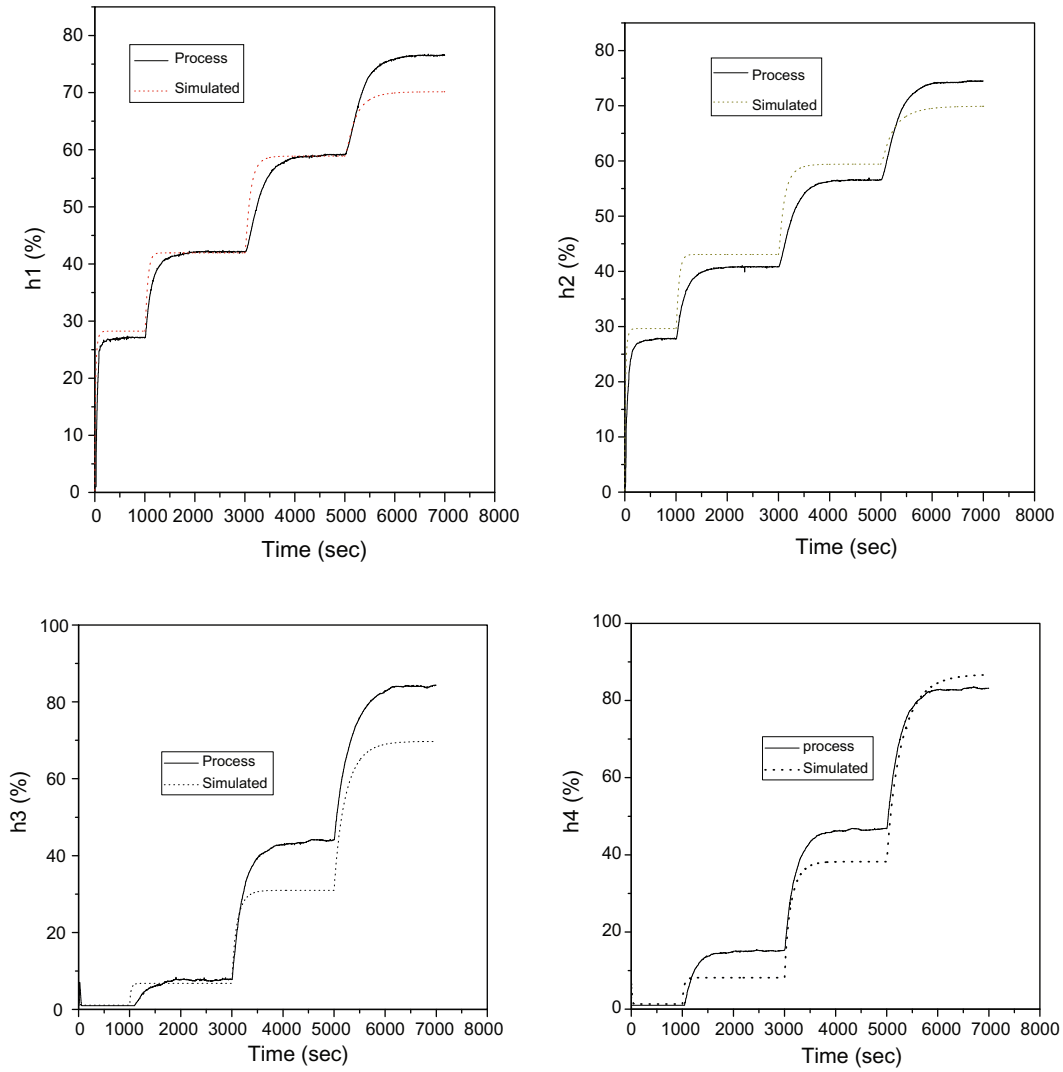

Fig. 5. Model validation.

4. Design of sliding mode controller

The standard normal form for a 2×2 multiple-input multiple-output (MIMO) process model is:

$$\begin{aligned} \dot{x}_1^1 &= x_2^1 \\ \dot{x}_2^1 &= \ddot{x}_1^1 = f_1^1(x) + g_1^1(x)u_1 + g_2^1 u_2 \\ \dot{x}_1^2 &= x_2^2 \\ \dot{x}_2^2 &= \ddot{x}_1^2 = f_1^2(x) + g_1^2(x)u_1 + g_2^2 u_2 \end{aligned} \tag{4.1}$$

where the complete dynamics of the system is represented by state vector $x = [x_1^1\ x_2^1\ x_1^2\ x_2^2]^T$. Output vector is $y = [x_1^1\ x_1^2]^T$. Superscripts used in above model stand for the respective output.

The model equations Eq. (3.2) needs to be transformed to the standard normal MIMO form for deducing the control law. Following assumptions were considered for representing the model equation in standard normal form.

Assumption 1. To achieve system stability and desired control performance, it only needs to control the levels of tank 3 and tank 4.

Remark 1. In the region of non-minimum phase, manipulated variables have very little effect on the levels of the bottom two tanks as their dynamics are mainly governed by the outflows coming from their respective top tanks. So for bottom two tanks, it can be presumed that the control actions are in their neighborhood of steady state values. Based on above, we propose the following theorem.

Theorem 1. *The sliding mode controller*

$$\begin{bmatrix} u_1 \\ u_2 \end{bmatrix} = \begin{pmatrix} \left(\frac{k_1' K_1 \gamma_1}{2\sqrt{h_1} A_1^2}\right) & \left(\frac{k_2' K_3}{2\sqrt{h_3} A_1 A_3}(1-\gamma_2)\right) \\ \left(\frac{k_1' K_4}{2\sqrt{h_4} A_2 A_4}(1-\gamma_1)\right) & \left(\frac{k_2' K_2 \gamma_2}{2\sqrt{h_2} A_2^2}\right) \end{pmatrix}^{-1} \times \left(\begin{pmatrix} -\lambda_1 sat(s_1) \\ -\lambda_2 sat(s_2) \end{pmatrix} - \begin{pmatrix} c_1 x_2^1 + \frac{K_1^2}{2A_1^2} - \frac{K_1 K_3 \sqrt{h_3}}{2A_1^2\sqrt{h_1}} - \frac{K_3^2}{2A_1 A_3} \\ c_2 x_2^2 + \frac{K_2^2}{2A_2^2} - \frac{K_2 K_4 \sqrt{h_4}}{2A_2^2\sqrt{h_2}} - \frac{K_4^2}{2A_2 A_4} \end{pmatrix} \right) \tag{4.2}$$

makes the system asymptotically stable to its desired values in presence of modeling uncertainty.

Proof. With the help of Assumption 1, the process model Eq. (3.2) can be rewritten as

$$\begin{aligned} A_1\dot{h}_1 &= -K_1\sqrt{h_1} + K_3\sqrt{h_3} + \gamma_1 k_1 u_{1o} \\ A_2\dot{h}_2 &= -K_2\sqrt{h_2} + K_4\sqrt{h_4} + \gamma_2 k_2 u_{2o} \\ A_3\dot{h}_3 &= -K_3\sqrt{h_3} + (1-\gamma_2)k_2 u_2 \\ A_4\dot{h}_4 &= -K_4\sqrt{h_4} + (1-\gamma_1)k_1 u_1 \end{aligned} \tag{4.3}$$

where u_{1o}, u_{2o} are the steady state operating values of manipulated variables.

The above model equation set is in standard normal form but this simplification creates uncertainty in system dynamics. These uncertainties can be termed as Δ. Except this some additional uncertainty comes into the system through the estimated values of K. Another important observation discussed in process model section was the variation of split fractions (γ values) with pump flow rates as depicted in Fig. 4. Instead of considering any variation in γ values, we keep it as constant. This reduces the order of controller model. We consider any additional uncertainty introduced by this is also lumped in Δ. The lumped parameter Δ is a total uncertainty vector. The regulation problem is now to be solved as a robust control problem. Sliding mode controller design is based on the fact that although the uncertainty is unknown, its upper bounds can be estimated and its effect can be eliminated by the switching action.

The resulting uncertain non-linear system dynamics can now be represented as

$$\begin{aligned} \dot{h}_1 &= \left(\frac{-K_1\sqrt{h_1} + K_3\sqrt{h_3} + \gamma_1 k_1 u_{1o}}{A_1}\right) + \Delta_1^1 \\ \dot{h}_3 &= \left(\frac{-K_3\sqrt{h_3} + (1-\gamma_2)k_2 u_2}{A_3}\right) + \Delta_2^1 \\ \dot{h}_2 &= \left(\frac{-K_2\sqrt{h_2} + K_4\sqrt{h_4} + \gamma_2 k_2 u_{2o}}{A_2}\right) + \Delta_1^2 \\ \dot{h}_4 &= \left(\frac{-K_4\sqrt{h_4} + (1-\gamma_1)k_1 u_1}{A_4}\right) + \Delta_2^2 \end{aligned} \tag{4.4}$$

Here we assume $\gamma_1 k_1 u_{1o} = k_1'$ and $\gamma_2 k_2 u_{2o} = k_2'$ as constant (the uncertainty term takes care of the error due to this) for obtaining proper relative degree. The uncertainty Δ_1^1 comes in the system from above consideration.

Remark 2. The Eq. (3.2) and the Eq. (4.4) both are very important here for finding out proper relative degree and actual control law. High degree of coupling and strong interconnection in the process can be observed here. The model seems to be simple but simple Lie algebraic operation does not able to come up with actual relative degree. Considering Eq. (3.2) alone the relative degree of the process becomes 1 which fails to incorporate effect higher order dynamics which is the most important here. Similarly considering (4.4) alone the relative degree criteria would have satisfied but actual control law may not be coming out properly. Omitting Eq. (3.2) the G matrix of Eq. (4.10) becomes right diagonal which would have failed to deduce actual control law. For avoiding those problem some tricky assumption is considered. Simplifying Eq. (3.2), (4.1), (4.2), (4.3), (4.4) a model uncertainty has raised whose effect is plugging up with the uncertainty term Δ_1^1. Now considering Eq. (4.4) brings uncertainty term Δ_1^1 which would have caused problem during coordinate transformation. So for maintaining coordinate transformation free from unknown term, the effect of Δ_1^1 is omitted here during transformation which gives a smooth coordinate transformation.

Now we apply the concept of feedback linearization of above model equation for output y_1=h_1 and y_2=h_2.Differentiating y_i we get,

$$\dot{y}_1 = \dot{x}_1^1 = \frac{\left(-K_1\sqrt{h_1} + K_3\sqrt{h_3} + k_1'\right)}{A_1} = x_2^1 \tag{4.5}$$

In Eq. (4.5) we omitted the term Δ_1^1 as we are trying to keep the coordinate transformation independent of unknown term (Remark 2).

As the feedback linearization condition is not yet met, Eq. (4.5) is further differentiated to yield

$$\begin{aligned} \dot{x}_2^1 &= \ddot{h}_1 \\ &= -\frac{K_1}{2A_1^2\sqrt{h_1}}\left(-K_1\sqrt{h_1} + K_3\sqrt{h_3} + \gamma_1 k_1 u_1\right) \\ &\quad + \frac{K_3}{2A_1A_3\sqrt{h_3}}\left(-K_3\sqrt{h_3} + (1-\gamma_2)k_2 u_2\right) \end{aligned} \tag{4.6}$$

Here Eq. (3.2) instead of Eq. (4.3) is used to express time derivatives (Remark 2). This will help us in calculating the proper relative degree of the process. As the relative degree criteria is fulfilled, we stop here and rearrange the above equation to get

$$\begin{aligned} \ddot{h}_1 &= \frac{K_1^2}{2A_1^2} - \frac{K_1K_3\sqrt{h_3}}{2A_1^2\sqrt{h_1}} - \frac{K_3^2}{2A_1A_3} + \left(-\frac{K_1\gamma_1 k_1}{2A_1^2\sqrt{h_1}}\right)u_1 \\ &\quad + \left(\frac{K_3k_2}{2A_1A_3\sqrt{h_3}}(1-\gamma_2)\right)u_2 + \Delta_2^1 \end{aligned} \tag{4.7}$$

Similar operation can be done for second output $y_2 = h_2 = x_1^2$ and this yields

$$x_2^2 = \dot{h}_2 = \left(\frac{-K_2\sqrt{h_2} + K_4\sqrt{h_4} + k_2'}{A_3}\right) \tag{4.8}$$

and

$$\begin{aligned} \dot{x}_2^2 = \ddot{h}_2 &= \frac{K_2^2}{2A_2^2} - \frac{K_2K_4\sqrt{h_4}}{2A_2^2\sqrt{h_2}} - \frac{K_4^2}{2A_2A_4} + \left(\frac{K_2k_2\gamma_2}{2A_2^2\sqrt{h_2}}\right)u_2 \\ &\quad + \left(\frac{K_4k_1}{2A_2A\sqrt{h_{4_4}}}(1-\gamma_1)\right)u_1 + \Delta_2^2 \end{aligned} \tag{4.9}$$

So the overall dynamics can be written as

$$\begin{bmatrix} \dot{x}_1^1 \\ \dot{x}_2^1 \\ \dot{x}_1^2 \\ \dot{x}_2^2 \end{bmatrix} = \underbrace{\begin{bmatrix} 0 & 1 & 0 & 0 \\ 0 & 0 & 0 & 0 \\ 0 & 0 & 0 & 1 \\ 0 & 0 & 0 & 0 \end{bmatrix}}_{A} \begin{bmatrix} x_1^1 \\ x_2^1 \\ x_1^2 \\ x_2^2 \end{bmatrix} + \underbrace{\begin{bmatrix} 0 & 0 \\ 1 & 0 \\ 0 & 1 \\ 0 & 0 \end{bmatrix}}_{B} \left[\underbrace{\begin{pmatrix} \frac{K_1^2}{2A_1^2} - \frac{K_1K_3\sqrt{h_3}}{2A_1^2\sqrt{h_1}} - \frac{K_3^2}{2A_1A_3} \\ \frac{K_2^2}{2A_2^2} - \frac{K_2K_4\sqrt{h_4}}{2A_2^2\sqrt{h_2}} - \frac{K_4^2}{2A_2A_4} \end{pmatrix}}_{F} + \underbrace{\begin{pmatrix} \frac{K_1k_1\gamma_1}{2\sqrt{h_1}A_1^2} & \frac{K_3}{2\sqrt{h_3}A_1A_3}(1-\gamma_2)k_2 \\ \frac{K_4k_1}{2\sqrt{h_4}A_2A_4}(1-\gamma_1) & \frac{K_2\gamma_2k_2}{2\sqrt{h_2}A_2^2} \end{pmatrix}}_{G} \right] \underbrace{\begin{bmatrix} u_1 \\ u_2 \end{bmatrix}}_{u} + \underbrace{\begin{bmatrix} \Delta_1^1 \\ \Delta_2^1 \\ \Delta_1^2 \\ \Delta_2^2 \end{bmatrix}}_{\Delta} \tag{4.10}$$

The above is in standard normal form as Eq. (4.1) where

$$\begin{aligned} x &= \begin{bmatrix} x_1^1 & x_2^1 & x_1^2 & x_2^2 \end{bmatrix}^T \\ &= \begin{bmatrix} h_1 & \left(\frac{(-K_1\sqrt{h_1}+K_3\sqrt{h_3}+k_1')}{A_1}\right)_1 & h_2 & \left(\frac{-K_2\sqrt{h_2}+K_4\sqrt{h_4}+k_2'}{A_3}\right) \end{bmatrix}^T \\ &\text{and} \quad y = [x_1^1 x_1^2]^T = [h_1 h_2]^T \end{aligned}$$

In more compact form we can represent our system as

$$\dot{z} = Az + B(F + Gu) + \Delta$$

The non-linear control law for stabilizing the nominal system is $u = G^{-1}(V - F)$.

The above simple feedback control law is valid when there is no significant amount of uncertainty present in the system. In presence of high magnitude of uncertainty, the control law may lead to unstable closed loop performance. Sliding mode control methodology is now employed to obtain robust performance even in presence of uncertainties.

Proper design of sliding surface makes the close loop dynamics restricted across the sliding surface. Whenever it tries to go beyond stability limit the switching action brings it back to the surface. Here we have a MIMO system, which will have more than one sliding surface for developing the control law.

Let us consider the sliding surfaces as

$$\begin{aligned} s_1 &= c_1 x_1^1 + x_2^1 \\ s_2 &= c_2 x_1^2 + x_2^2 \end{aligned} \tag{4.11}$$

To ensure stability, the controller will force the condition: $s\dot{s} < 0$

Now differentiating Eq. (4.11) we get

$$\begin{aligned} \dot{s}_1 &= c_1 \dot{x}_1^1 + \dot{x}_2^1 \\ &=> c_1 x_2^1 + \frac{K_1^2}{2A_1^2} - \frac{K_1 K_3 \sqrt{h_3}}{2A_1^2\sqrt{h_1}} - \frac{K_3^2}{2A_1 A_3} + \left(\frac{K_1 \gamma_1 k_1}{2\sqrt{h_1} A_1^2}\right) u_1 \\ &\quad + \left(\frac{K_3 k_2}{2\sqrt{h_3} A_1 A_3}(1-\gamma_2)\right) u_2 + \Delta_2^1 + c_1 \Delta_1^1 \end{aligned} \tag{4.12}$$

$$\begin{aligned} \dot{s}_2 &= c_2 \dot{x}_1^2 + \dot{x}_2^2 \\ &=> c_2 x_2^2 + \frac{K_2^2}{2A_2^2} - \frac{K_2 K_4 \sqrt{h_4}}{2A_2^2\sqrt{h_2}} - \frac{K_4^2}{2A_2 A_4} + \left(\frac{K_2 \gamma_2 k_2}{2\sqrt{h_2} A_2^2}\right) u_2 \\ &\quad + \left(\frac{K_4 k_1}{2\sqrt{h_4} A_2 A_4}(1-\gamma_1)\right) u_1 + \Delta_2^2 + c_2 \Delta_1^2 \end{aligned} \tag{4.13}$$

The above equations can be expressed together as

$$\begin{bmatrix} s_1\dot{s}_1 \\ s_2\dot{s}_2 \end{bmatrix} = \begin{bmatrix} s_1\left(c_1 x_2^1 + \frac{K_1^2}{2A_1^2} - \frac{K_1K_3\sqrt{h_3}}{2A_1^2\sqrt{h_1}} - \frac{K_3^2}{2A_1A_3} + \left(\frac{K_1k_1\gamma_1}{2\sqrt{h_1}A_1^2}\right)u_1 + \left(\frac{K_3k_2}{2\sqrt{h_3}A_1A_3}(1-\gamma_2)\right)u_2 + \Delta_2^1 + c_1\Delta_1^1\right) \\ s_2\left(c_2 x_2^2 + \frac{K_2^2}{2A_2^2} - \frac{K_2K_4\sqrt{h_4}}{2A_2^2\sqrt{h_2}} - \frac{K_4^2}{2A_2A_4} + \left(\frac{K_2k_2\gamma_2}{2\sqrt{h_2}A_2^2}\right)u_2 + \left(\frac{K_4k_1}{2\sqrt{h_4}A_2A_4}(1-\gamma_1)\right)u_1 + \Delta_2^2 + c_2\Delta_1^2\right) \end{bmatrix} \tag{4.14}$$

Now we do not have much information of the uncertainty term Δ before hand but its bound can be assumed. In order to estimate a worst case bound on the function Δ the following assumption is considered:

Assumption 2. There exists a known function η such that $\|\Delta\| \leqslant \eta(h,t)$.

Where $\eta(h,t)$ is a non-negative and continuous known function and it can be well approximated by proper prediction of uncertainty bounds in the system.

$$\begin{aligned} |\Delta_1^1| &\leqslant \eta_1^1 \leqslant \max\left(10\left(\frac{(-K_{1o}\sqrt{h_1} + K_{3o}\sqrt{h_3})}{A_1}\right), 0\right) \\ |\Delta_2^1| &\leqslant \eta_2^1 \leqslant \max\left(5\left(\frac{K_{1o}^2}{2A_1^2} - \frac{K_{1o}K_{3o}\sqrt{h_3}}{2A_1^2\sqrt{h_1}} - \frac{K^2}{2A_1A_3} \right.\right. \\ &\qquad \left.\left. + \left(\frac{k_1K_{1o}}{2\sqrt{h_1}A_1^2}\right)u_{1o} + \left(\frac{k_2K_{3o}}{2\sqrt{h_3}A_1A_3}\right)u_{2o}\right), 0\right) \\ |\Delta_1^2| &\leqslant \eta_1^2 \leqslant \max\left(10\left(\frac{(-K_{2o}\sqrt{h_2} + K_{4o}\sqrt{h_4})}{A_2}\right), 0\right) \\ |\Delta_2^2| &\leqslant \eta_2^2 \leqslant \max\left(5\left(\frac{K_{2o}^2}{2A_2^2} - \frac{K_{2o}K_{4o}\sqrt{h_4}}{2A_2^2\sqrt{h_2}} - \frac{K_{4o}^2}{2A_2A_4} \right.\right. \\ &\qquad \left.\left. + \left(\frac{k_2K_{2o}}{2\sqrt{h_2}A_2^2}\right)u_{2o} + \left(\frac{k_1K_{4o}}{2\sqrt{h_4}A_2A_4}\right)u_{1o}\right), 0\right) \end{aligned} \tag{4.15}$$

where $K_{1o} = K_{2o} = K_{3o} = K_{4o} = 10$ and $u_{1o} = u_{2o} = 50$ are the nominal values. Since the write hand side of Eq. (4.15) is considered as maximum possible uncertainty, Eq. (4.14) can be written in an inequality form.

$$\begin{aligned} \begin{bmatrix} s_1\dot{s}_1 \\ s_2\dot{s}_2 \end{bmatrix} \leqslant \begin{bmatrix} s_1 & 0 \\ 0 & s_2 \end{bmatrix} \Bigg[& \begin{pmatrix} c_1x_2^1 + \frac{K_1^2}{2A_1^2} - \frac{K_1K_3\sqrt{h_3}}{2A_1^2\sqrt{h_1}} - \frac{K_3^2}{2A_1A_3} \\ c_2x_2^2 + \frac{K_2^2}{2A_2^2} - \frac{K_2K_4\sqrt{h_4}}{2A_2^2\sqrt{h_2}} - \frac{K_4^2}{2A_2A_4} \end{pmatrix} \\ & + \begin{pmatrix} \left(\frac{k_1K_1\gamma_1}{2\sqrt{h_1}A_1^2}\right) & \left(\frac{k_2K_3}{2\sqrt{h_3}A_1A_3}(1-\gamma_2)\right) \\ \left(\frac{k_1K_4}{2\sqrt{h_4}A_2A_4}(1-\gamma_1)\right) & \left(\frac{k_2K_2\gamma_2}{2\sqrt{h_2}A_2^2}\right) \end{pmatrix} \begin{pmatrix} u_1 \\ u_2 \end{pmatrix} \\ & + \begin{pmatrix} |\eta_2^1| + c_1|\eta_1^1| \\ |\eta_2^2| + c_2|\eta_1^2| \end{pmatrix} \Bigg] \end{aligned} \tag{4.16}$$

substituting

$$\begin{aligned} & \begin{pmatrix} c_1x_2^1 + \frac{K_1^2}{2A_1^2} - \frac{K_1K_3\sqrt{h_3}}{2A_1^2\sqrt{h_1}} - \frac{K_3^2}{2A_1A_3} \\ c_2x_2^2 + \frac{K_2^2}{2A_2^2} - \frac{K_2K_4\sqrt{h_4}}{2A_2^2\sqrt{h_2}} - \frac{K_4^2}{2A_2A_4} \end{pmatrix} \\ & + \begin{pmatrix} \left(\frac{k_1K_1\gamma_1}{2\sqrt{h_1}A_1^2}\right) & \left(\frac{k_2K_3}{2\sqrt{h_3}A_1A_3}(1-\gamma_2)\right) \\ \left(\frac{k_1K_4}{2\sqrt{h_4}A_2A_4}(1-\gamma_1)\right) & \left(\frac{k_2K_2\gamma_2}{2\sqrt{h_2}A_2^2}\right) \end{pmatrix} \begin{pmatrix} u_1 \\ u_2 \end{pmatrix} = \begin{bmatrix} v_1 \\ v_2 \end{bmatrix} \end{aligned}$$

in above we get

$$\Rightarrow \begin{bmatrix} s_1\dot{s}_1 \\ s_2\dot{s}_2 \end{bmatrix} \leqslant \begin{bmatrix} s_1 & 0 \\ 0 & s_2 \end{bmatrix} \left[\begin{pmatrix} v_1 \\ v_2 \end{pmatrix} + \begin{pmatrix} |\eta_2^1| + c_1|\eta_1^1| \\ |\eta_2^2| + c_2|\eta_1^2| \end{pmatrix} \right] \tag{4.17}$$

or

$$\Rightarrow \begin{bmatrix} s_1\dot{s}_1 \\ s_2\dot{s}_2 \end{bmatrix} \leqslant \begin{bmatrix} s_1 & 0 \\ 0 & s_2 \end{bmatrix} \left[\begin{pmatrix} v_1 \\ v_2 \end{pmatrix} + \begin{pmatrix} \eta_1' \\ \eta_2' \end{pmatrix} \right] \tag{4.18}$$

where

$$\begin{pmatrix} \eta_1' \\ \eta_2' \end{pmatrix} = \begin{pmatrix} |\eta_2^1| + c_1|\eta_1^1| \\ |\eta_2^2| + c_2|\eta_1^2| \end{pmatrix}$$

where sliding action v would be

$$v = -\lambda \operatorname{sign}(s) \tag{4.19}$$

where $\lambda_1 > \eta_1' \lambda_2 > \eta_2'$.

Substituting this Eq. (4.20) now becomes

$$\begin{bmatrix} s_1\dot{s}_1 \\ s_2\dot{s}_2 \end{bmatrix} < \left[\begin{pmatrix} s_1(\eta_1' - \lambda_1 sign(s_1)) \\ s_2(\eta_2' - \lambda_2 sign(s_2)) \end{pmatrix} \right] \tag{4.20}$$

For any values of s_1, s_2 the above equation can be represented as

$$\begin{bmatrix} s_1\dot{s}_1 \\ s_2\dot{s}_2 \end{bmatrix} < \begin{pmatrix} 0 \\ 0 \end{pmatrix} \tag{4.21}$$

The control action generated by sign(x) is for bringing back the process on the stable sliding surface and this drastic action at times result in chattering of the controller output. To reduce this undesirable chattering, a boundary layer is considered around the sliding surface within which this control action is implemented by a continuous saturating function sat(x). Using sat(x) instead of sign(x) reduces chattering.

$$\mathrm{sat}(x) = \begin{cases} \mathrm{sign}(x) & \text{if } |x| > 1 \\ \mathrm{sign}(x) & \text{if} |x| > 1 \end{cases} \tag{4.22}$$

So the final control law takes the form of Eq. (4.2):

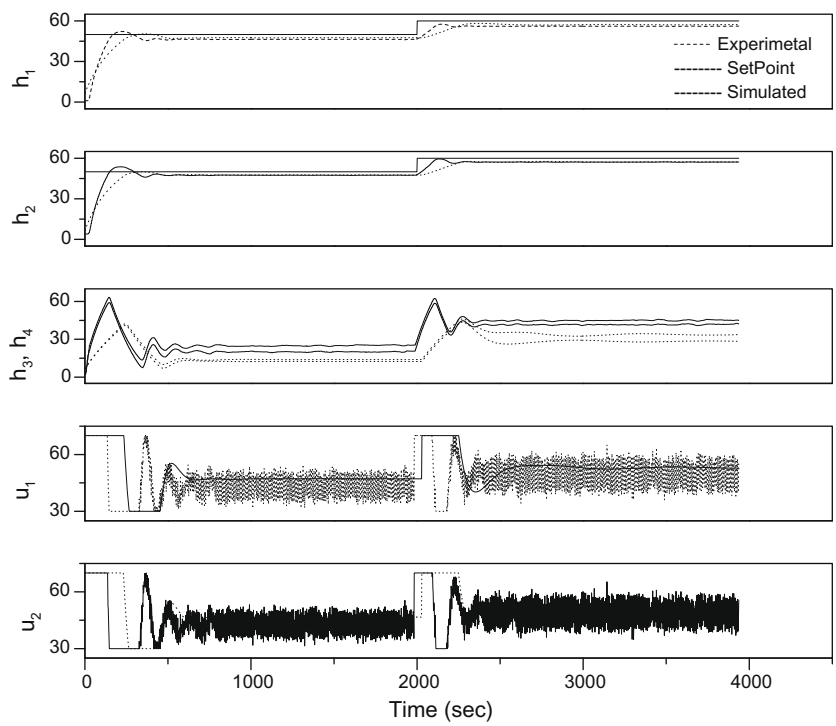

Fig. 6. Decentralized PI controller performance.

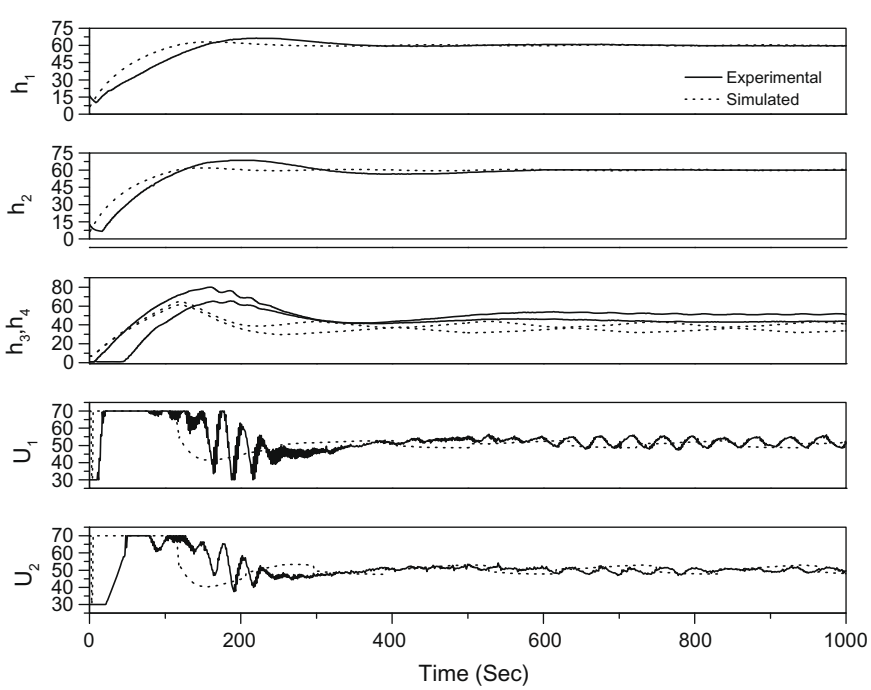

Fig. 7. Sliding mode controller without boundary layer performance.

The inequality (4.21) holds well enough through out the operation. The outputs reach their desire values within finite time. The sliding gain (λ) can be adjusted to accelerate this. In present work the value of λ is considered as (100, 100) and the boundary layer thickness is 0.1. Therefore it can be concluded that outputs asymptotically converge to desired values within acceptable time. The proposed controller combines feedback linearization and sliding mode algorithm, is robust to model uncertainties and is stable. Performance of the controller is described in next section.

Remark 3. The state variables are always working between maximum and minimum limit. For all tanks the heights are varying from 0.03 cm to 30 cm. Manipulated variables are also varying within the limits. It can be clearly observed from any figures

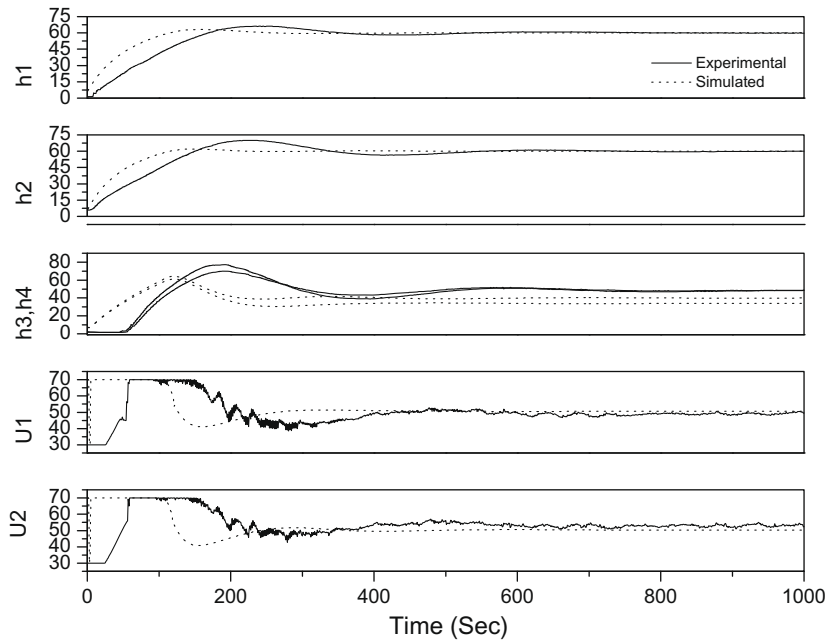

Fig. 8. Sliding mode controller with boundary layer performance.

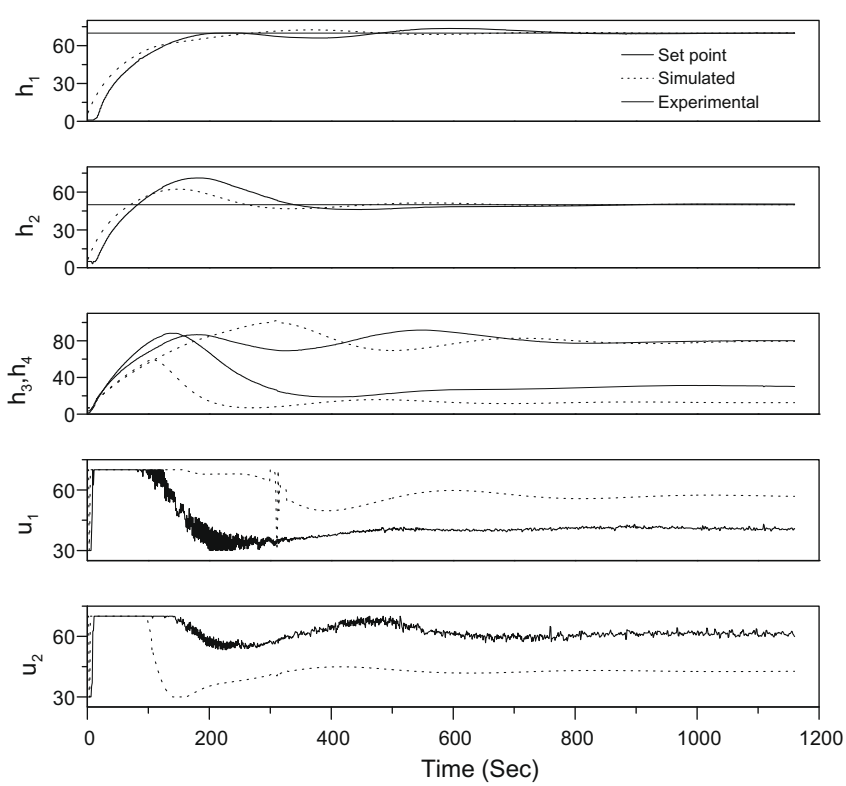

Fig. 9. Sliding mode control for set point trajectory I.

starting from 6. From those figures it is clearly observed that all the state variables and the manipulated variables are operating within limits. The controller is robust enough to eliminate the saturation problem also. As Other parameters in the inverse term are constant, so within the limits the matrix in Eq. (4.2) is always invertible.

5. Results and discussion

Results of application of the sliding mode controller on the simulated as well as the real process are discussed in this section. All the results have manipulated variables or state variables as % of their respective range.

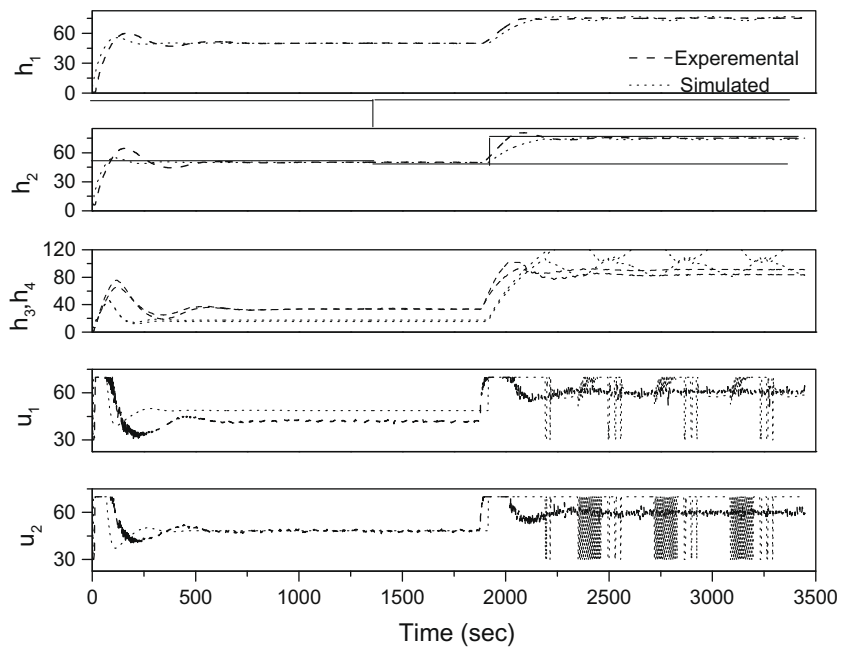

Fig. 10. Sliding mode control with for set point trajectory II.

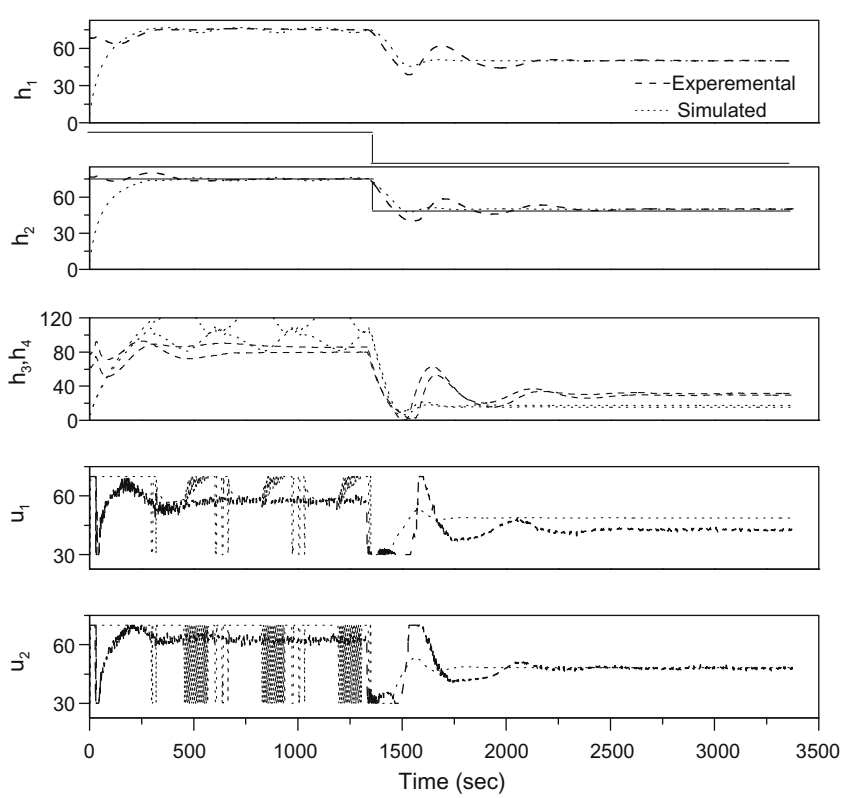

Fig. 11. Sliding mode control for setpoint trajectory III.

Performance of controller can be judged from (1) closeness of the set point trajectory and the controlled variable response, (2) time to stabilize to the new steady state (3) robustness to disturbances/load changes, and (4) chattering/fluctuations in controller output. Normally these performances are observed from an initial steady state to another or around a steady state. A more strict con-

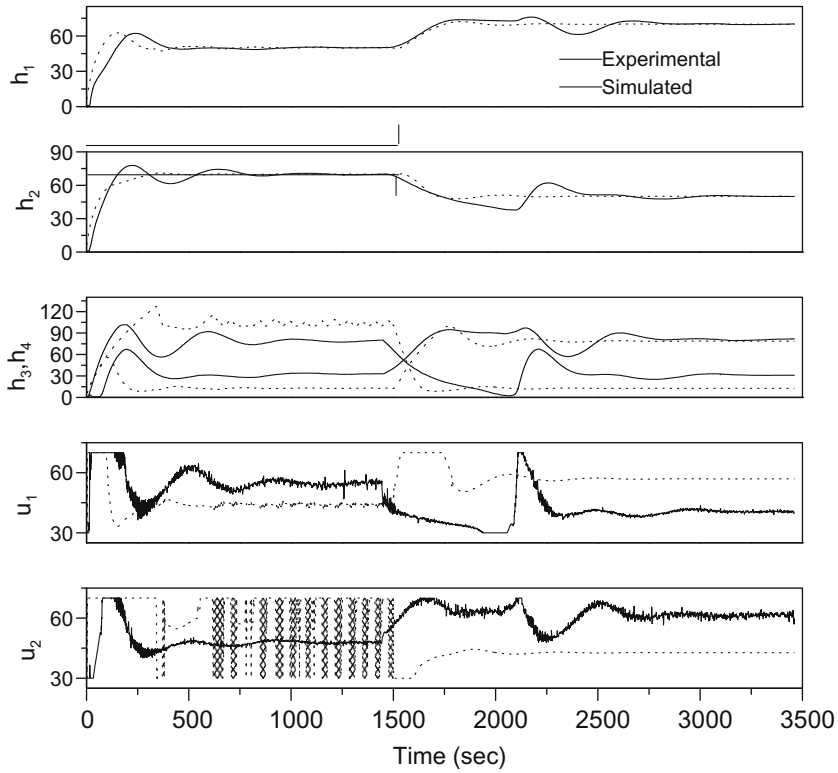

Fig. 12. Sliding mode controller performance for set point trajectory IV.

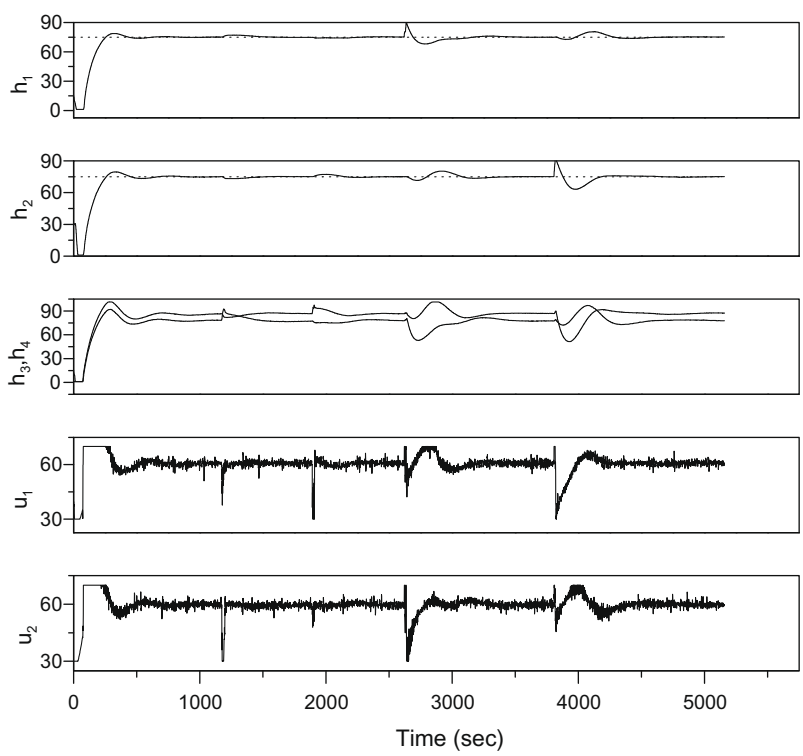

Fig. 13. Sliding mode controller performance for disturbance.

dition is enforced in some of our experiments where initial vales of h_1/h_2 start from zero, i.e. beyond the stable range of operation of the system.

5.1. Performance of individual PI control of levels (h_1 and h_2)

PI controller scheme for the process is shown in Fig. 6. The controllers are designed around the operating point [(h_1 h_2 h_3 h_4 u_1 u_2) = (50 50 50 50 55 55)] and their tuning constants (K_c = 100 and 300, T_i = 150 and 400) are determined by direct synthesis method. Step responses of the closed loop PI controllers are shown here both for the simulated as well as the real process. The simulated process behavior matches the real process quite closely. It takes close to 500 sec to reach the set point value of 50% level from 0% level. After stabilization at 50% level, set point step change to 70% is imposed. It takes close to 200 s for the process to stabilize again. We can see that there is a steady state offset present that we could not eliminate without introducing excessive fluctuation in the manipulated variable.

5.2. Performance comparison: sliding mode controller and sliding mode controller with boundary layer

The performance of sliding mode controller without the boundary layer for normal set point trajectory is shown in Fig. 7. It is seen that even after h_1 and h_2 stabilizes, oscillations persist in h_3 and h_4 values. These oscillations in h_3 and h_4 affect flows to tanks 1 and 2 and to control their levels (h_1 and h_2), the controller takes action and leads to the undesirable chattering in the manipulated variables. Performance of the controller with the boundary layer is shown in Fig. 8. Here, we have maintained the thickness of boundary layer at 0.1. The chattering effect is reduced with favorable effect on life of final control element.

5.3. Performance of sliding mode controller with boundary layer

From Fig. 9 onwards we have presented performance of sliding mode controller with boundary layer. Unless otherwise stated, sliding mode controller is henceforth synonymous to sliding mode controller with boundary layer.

Results of servo problem of achieving 70% and 50% for h1 and h2, starting initially from 0% level in the two bottom tanks is shown in Fig. 9. The tracking performance is quiet good for both simulated as well as the real system. It takes around 500 s to reach the desired set points. Also the manipulated variable chattering dies down quickly.

In Fig. 10 results of a further set point step change are presented. In this case both the set points for h_1 and h_2 are changed from steady state at t = 2000 s, from 50% to 75%. The set point tracking is found to be satisfactory both for the simulated as well as the real process. The controller has satisfactory performance at lower set point without any visible chattering in controller output.

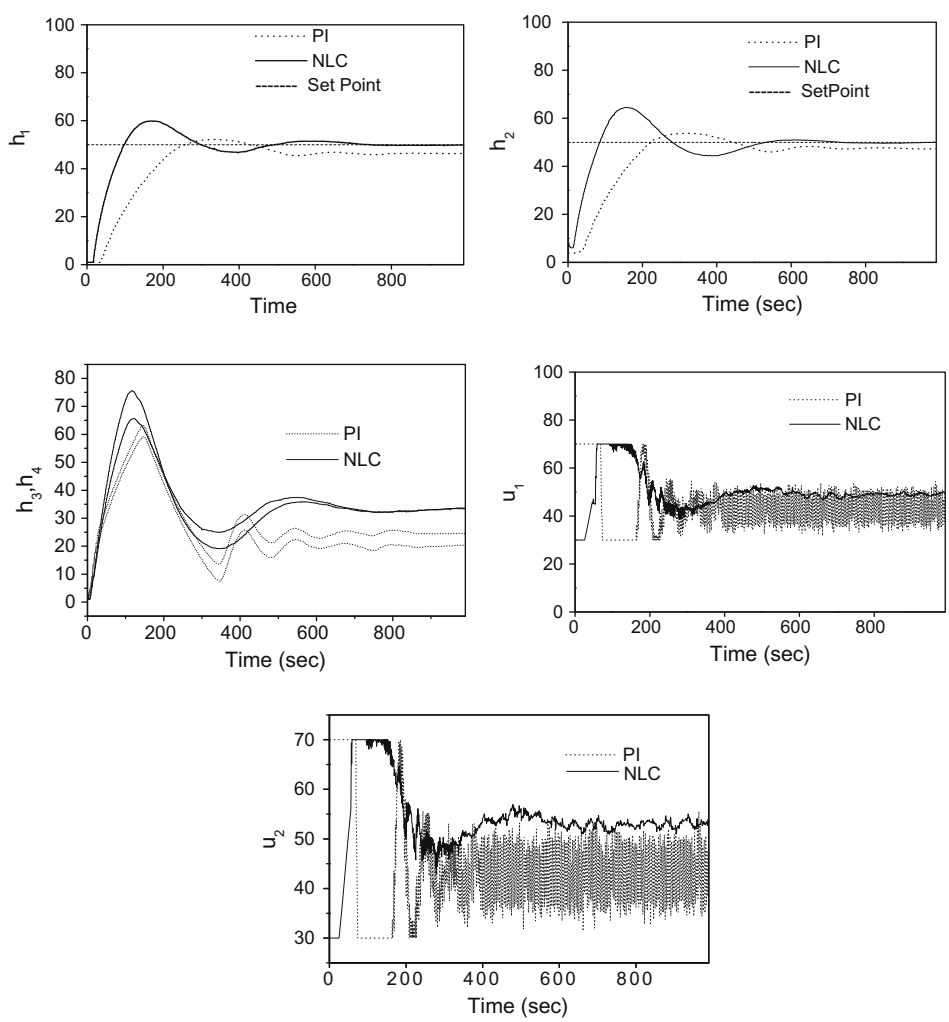

Fig. 14. Comparison of performance of normal PI controller with sliding mode control with BL (servo problem).

As the controlled variables reach higher values (i.e. around 65–75%), chattering in manipulated variables are observed. As the system rolls closer to towards non-minimum phase at higher pump outputs (Fig. 4), more frequent control actions bring back the system trajectory to the sliding surface.

Results of exactly reverse case of set point changes are shown in Fig. 11. The initial set points are 75%, and finally at $t = 2000$ s, from steady state, both set points are stepped down to 50%. The upper tanks (h_3 and h_4) touch a close to dry out condition soon after the set points changes are imposed. As this happens, controller responses chatter, trying to get the system back to the stable sliding surface. The controller is observed to stabilize the system and attain regulation within 200 s.

In Fig. 12, we find the results of different step changes in set points for h_1 and h_2. Set point of h_1 changes from 50% to 70% and for h_2 it is 70–50% implemented at $t = 1500$ s, when the system was fairly steady. The changes in manipulated variables in opposite direction perturb the coupled 2×2 MIMO system drastically. To meet the control objective more flow is needed into tank 1, which the controller tries to ensure by increasing % output of pump 1 and sending more direct flow to the tank. Simultaneously, the flow through pump 2 is cut back to reduce direct flow to tank 2 and make its level track corresponding set point reduction from 70% to 50%. Reduction in pump 2 flow lowers (direct) water flow rate to tank 3 that in turn works to reduce level in tank 1. This destabilizing effect comes like a disturbance into the system and is the result of strong interaction between the process variables. The controller tackles this and takes almost 1000 s to reach the process finally quite close to its new regulatory target values.

Results of response of the controller to disturbances introduced to the system are presented in Fig. 13. Sudden addition of a quantity of water to any of the tank provides the equivalent of impulse disturbance. In a single experiment four disturbances have been introduced one after another. At $t = 1000$ s water equivalent to 5% level rise is added in tank 3. The controller is seen to reject this disturbance effect and h_1 and h_2 are hardly affected. At $t = 2000$ s, water equivalent to 5% level rise is added in tank 4. This disturbance is also rejected equally efficiently. At $t = 2500$ s, water equivalent to 10% level rise is added in tank 1 and the controller takes around 1000 s to reject its effect and gain back regulation. The actions of controller lead to relatively large fluctuations in tank 3 and tank 4 levels. At $t = 3800$ s water equivalent to 10% level rise is added in tank 2. Responses shown prove good disturbance rejection in this case also. The foregoing results illustrate the robustness of the controller in presence of reasonable magnitude of disturbances.

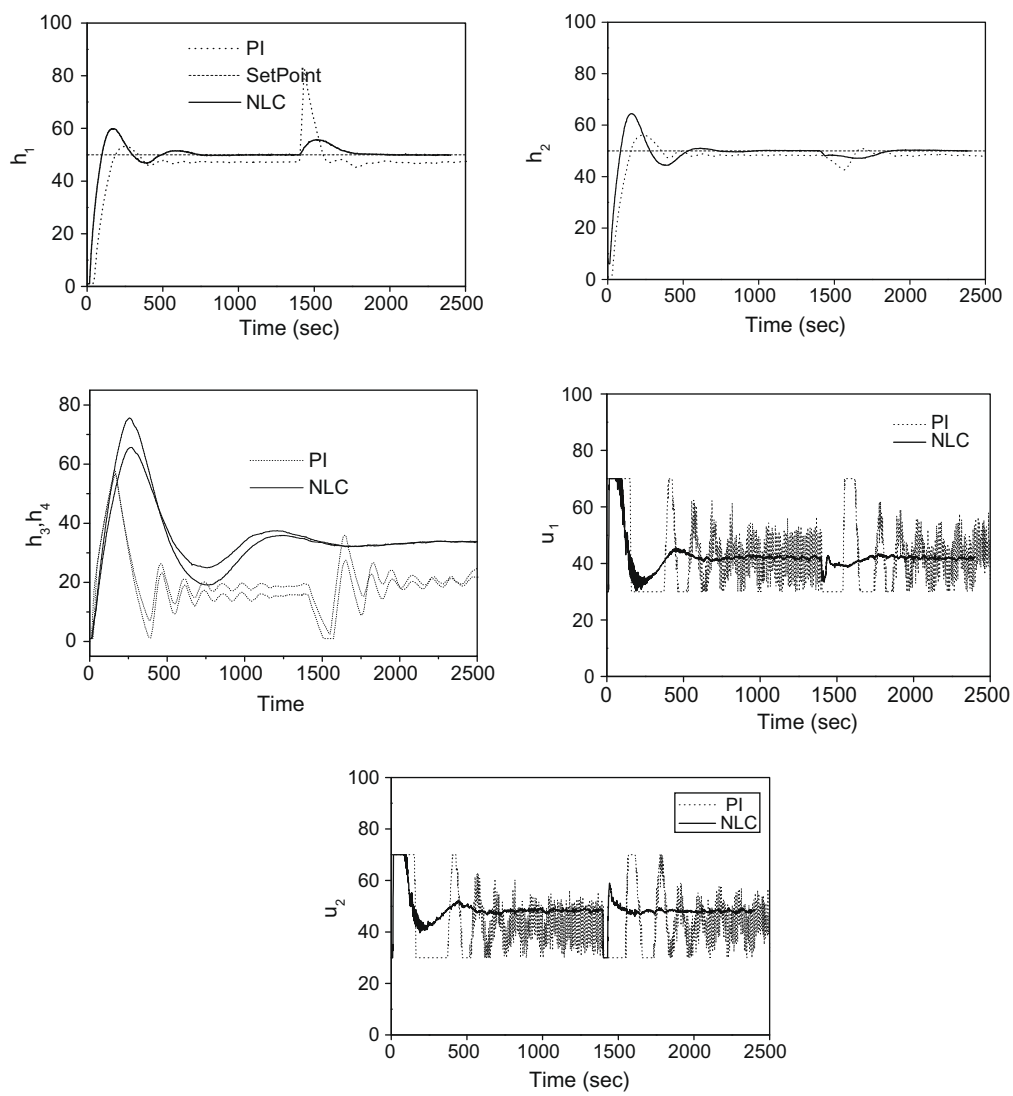

Fig. 15. Comparison of normal PI controller performance with sliding mode control (regulatory problem).

5.4. Comparison of sliding mode and PI controller performance on real process

Fig. 14 shows the comparative servo control results of PI controller and sliding mode controller. The controller attempts to reach the target set points. Here we find PI control leads to undesirable chattering of controller outputs. Also there is offset and the initial speed of response for PI controller is slower compared to sliding mode control.

The comparative regulatory performance of PI and sliding mode control is shown in Fig. 15. A pulse disturbance to the system is introduced by manually plugging the drain valve from tank 1 for 10 s. The sliding mode controller outperforms PI in this case also with lower peak deviation from set point, much quicker disturbance rejection as well as negligible chattering of controller outputs.

The step-by-step design of the sliding mode controller with incorporation of boundary layer leads to a robust controller with good regulatory performance as well as low chattering for the complex quadruple tank problem. This controller outperforms the PI controllers on all accounts.

6. Conclusion

Sliding mode control algorithm has been used to control the quadruple tank process in its narrow zone of stability where the system has non-minimum phase behavior. In spite of experimentally establishing that split fractions change with operating conditions and affects transmission zero locations, the control algorithm uses constant value of split fraction to keep the controller model order low. This uncertainty is found to be easily handled by the sliding mode control algorithm. The non-linear controller outperforms the PI controller for both servo and regulatory performances. The propose controller is also robust to disturbances.

References

[1] Khan MK, Spurgeonm SK. Robust MIMO water level control in interconnected twin tanks using second order sliding mode control. Control Eng Pract J 2006;14:375–86.
[2] Pan H, Wong H, Kapila V, de Queiroz MS. Experimental validation of a nonlinear backstepping liquid level controller for a state coupled two tank system. Control Eng Pract J 2005;13:27–40.
[3] Kwork KE, Ping MC, Li P. A model based augmented PID algorithm. J. Process Control 2000;10:9–18.
[4] Wu KL, Yu CC, Cheng YC. A two degree of freedom level control. J Process Control 2001;11:311–9.
[5] Tan KK, Huang S, Ferdous R. Robust self-tuning PID controller for nonlinear systems. J. Process Control. 2002;12:753–61.
[6] Murray-Smith DJ, Kocijan J, Gong M. A signal convolution method for estimation of controller parameter sensitivity functions for tuning of feedback control systems by an iterative process. Control Eng Pract J 2003;11:1087–94.
[7] Johansson KH. Relay feedback and multivariable control. PhD thesis, Department of Automatic Control, Lund Institute of Technology, Sweden; November 1997.
[8] Johansson KH. The quadruple tank process – a multivariable laboratory process with an adjustable zero. IEEE Trans Control Syst Tech J 2000;8(3).
[9] Grebeck M. A comparison of controllers for the quadruple tank system. Department of Automatic Control, Lund Institute of Technology, Lund, Sweden, Tech. rep., 1998.
[10] Johansson KH, Horch A, Hansson A. Teaching multivariable control using the quadruple tank process. In: Proceeding of the 38th conference on decision & control; December 1999.
[11] Johansson KH, James B, Bryant GF, Astrom KJ. Multivariable controller tuning. In: 17th Amer. Contr. Conf. Philadelphia PA; 1998.
[12] Recica V. Automatic tuning of multivariable controllers. Master thesis, Dept. Automat. Contr., Lund Inst. Technol., Lund, Sweden; 1998.
[13] Utkin VI. Variable structure systems with sliding modes. IEEE Trans Automat Control 1977;AC-22:212–22.
[14] Decarlo RA, Zak SH, Mathews GP. Variable structure control of nonlinear systems: a tutorial. Proc IEEE 1988;76:212–32.
[15] Utking VI. Sliding modes in control and optimization. Berlin: Springer-Verlag; 1992.
[16] Bartolinin G, Zolezzi T. Variable structure systems nonlinear in the control law. IEEE Trans Automat Control 1985;30:681–4.
[17] Zinober ASI. Variable structure and Lyapunov control. Berlin: Springer-Verlag; 1994.
[18] Li THS, Kuo CL, Guo NR. Design of an EP-based fuzzy sliding-mode control for a magnetic ball suspension system. Chaos Solitons Fract J 2007;33:1523–31.
[19] Lino P, Maione B, Rizzo A. Nonlinear modeling and control of a common rail injection system for diesel engines. Appl Math Model J 2007;31:1770–84.
[20] Iglesias E, García Y, Sanjuan M, Camacho O, Smith C. Fuzzy surface-based sliding mode control. ISA Trans J 2007;46:73–83.
[21] Chen CT, Peng ST. A sliding mode control scheme for non-minimum phase non-linear uncertain input-delay chemical processes. J Process Control 2006;16:37–51.
[22] Yound KD, Utkin VI, Ozguner U. A control engineer's guide to sliding mode control. IEEE Trans Control Syst Technol J 1999;7(3):328–42.
[23] Almutairi NB, Zribi M. Sliding mode control of coupled tanks. Mechatronics J 2006;16:427–41.